

Ab initio Molecular Dynamics of H₂ Dissociative Adsorption on Graphene Surfaces

Kentaro Doi^{1,2}, Ikumi Onishi¹ and Satoyuki Kawano^{1,3}

Abstract: Hydrogen technologies are currently one of the most actively researched topics. A lot of researches have tried to enhance their energy conversion efficiencies. In the present study, numerical analyses have been carried out focusing on hydrogen-storage carbon materials which are expected to realize high gravimetric and volumetric capacities. In particular, dissociative adsorption processes of H₂ molecules above graphene surfaces have been investigated by *ab initio* molecular dynamics. The present results indicate that a steric graphene surface plays an important role in enhancing the charge transfer which induces dissociation of H₂ and adsorption of H atoms on the surface. The dissociation energy required for the reaction $\text{H}_2 \rightarrow 2\text{H}$ above the steric sites is expected to be reduced to 56.2 % of that in vacuum without graphene. Thus, distorted graphenes are an effective hydrogen-storage material, which functions as a catalytic agent.

Keywords: *Ab initio* MD, Graphene, Hydrogen storage, Dissociative adsorption

1 Introduction

Recently, hydrogen technologies have received considerable interest as a means of producing clean and safe power supplies. However, several problems, such as portability, safety, and cost performance, have to be solved to realize so-called hydrogen economy. Carbon nanomaterials are one of the most promising candidates for hydrogen-storage materials due to their low weight and high cost performance, compared with other metallic alloys [Dillon, Jones, Bekkedahl, Kiang, Bethune, and Heben (1997); Chen, Wu, Lin, and Tan (1999); Elias, Nair, Mohiuddin, Morozov, Blake, Halsall, Ferrari, Boukhvalov, Katsnelson, Geim, and

¹ Department of Mechanical Science and Bioengineering, Graduate School of Engineering Science, Osaka University, Osaka 560-8531, Japan

² doi@me.es.osaka-u.ac.jp

³ kawano@me.es.osaka-u.ac.jp

Novoselov (2009); Berseth, Harter, Zidan, Blomqvist, Araújo, Scheicher, Ahuja, and Jena (2009); Guisiner, Rutter, Crain, First, and Stroschio (2009); Riedl, Coletti, Iwasaki, Zakharov, and Starke (2009); Riedl, Coletti, and Starke (2010); Virojanadara, Yakimova, Zakharov, and Johansson (2010); Virojanadara, Zakharov, Yakimova, and Johansson (2010); Liu, Fan, Liu, Cong, Cheng, and Dresselhaus (1999); Ströbel, Jörissen, Schliermann, Trapp, Schütz, Bohmhammel, Wolf, and Garche (1999); Yang (2000); Gupta and Srivastava (2000, 2001); Hirscher, Becher, Haluska, Dettlaff-Weglikowska, Quintel, Duesberg, Choi, Downes, Hulman, Roth, Stepanek, and Bernier (2001); Chen, Shaw, Bai, Wang, Lund, Lu, and Chung (2001); Nishimiya, Ishigaki, Takikawa, Ikeda, Hibi, Sakakibara, Matsumoto, and Tsutsumi (2002); Xu, Takahashi, Matsuo, Hattori, Kumagai, Ishiyama, Kaneko, and Iijima (2007)]. A few pioneering experimental studies on hydrogen-chargeable carbon materials have been performed [Dillon, Jones, Bekkedahl, Kiang, Bethune, and Heben (1997); Chen, Wu, Lin, and Tan (1999)], and recent reports indicate that graphene is preferable materials for hydrogen storages [Elias, Nair, Mohiuddin, Morozov, Blake, Halsall, Ferrari, Boukhvalov, Katsnelson, Geim, and Novoselov (2009); Berseth, Harter, Zidan, Blomqvist, Araújo, Scheicher, Ahuja, and Jena (2009); Guisiner, Rutter, Crain, First, and Stroschio (2009); Riedl, Coletti, Iwasaki, Zakharov, and Starke (2009); Riedl, Coletti, and Starke (2010); Virojanadara, Yakimova, Zakharov, and Johansson (2010); Virojanadara, Zakharov, Yakimova, and Johansson (2010)]. It is suggested that distorted surfaces and curvatures of carbon materials play a significant role in hydrogen storage technologies [Elias, Nair, Mohiuddin, Morozov, Blake, Halsall, Ferrari, Boukhvalov, Katsnelson, Geim, and Novoselov (2009); Berseth, Harter, Zidan, Blomqvist, Araújo, Scheicher, Ahuja, and Jena (2009)]. In addition, novel properties of graphene layers fabricated on SiC substrates have also attracted attentions [Berseth, Harter, Zidan, Blomqvist, Araújo, Scheicher, Ahuja, and Jena (2009); Guisiner, Rutter, Crain, First, and Stroschio (2009); Riedl, Coletti, Iwasaki, Zakharov, and Starke (2009); Riedl, Coletti, and Starke (2010); Virojanadara, Yakimova, Zakharov, and Johansson (2010); Virojanadara, Zakharov, Yakimova, and Johansson (2010)]. In those works, it is reported that hydrogen adsorption and desorption properties are expressed at the interface of graphenes and SiC substrates by the peculiar electronic properties. Theoretical investigations have featured interactions between hydrogen species and carbon nanomaterials, such as carbon nanotubes (CNTs) [Tada, Furuya, and Watanabe (2001); Miura, Kasai, Diño, Nakanishi, and Sugimoto (2003); Nakano, Ohta, Yokoe, Doi, and Tachibana (2006); Doi, Nakano, Ohta, and Tachibana (2007); Durgun, Ciraci, and Yildirim (2008); Hanasaki, Nakamura, Yonebayashi, and Kawano (2008); Cheng, Pez, Kern, Kresse, and Hafner (2001)], carbon nanofibers [Chan, Chen, Gong, and Liu (2001); Li, Furuta, Goto, Ohashi, Fujiwara, and Yip (2003); Cheng, Pez, and Cooper (2003)], and graphenes [Jeloacia and Sidis (1999); Arel-

lano, Molina, Rubio, and Alonso (2000); Okamoto and Miyamoto (2001); Sha and Jackson (2001); Patchkovskii, Tse, Yurchenko, Zhechkov, Heine, and Seifert (2005)]. They reported that surface distortions cause carbon networks to change their bonding states. However, most *ab initio* studies are based on static mechanics of H atoms due to the mathematical difficulty and huge computational cost of modeling dynamic processes of H₂ molecules.

In the present study, a technique for dynamic analysis on reaction systems is developed, based on a coupling procedure of *ab initio* methods and molecular dynamics (MD) for parallel computing. Here, *ab initio* MD computations are effectively used to determine a condition which permits dissociative adsorption of H₂ above graphene surface and to find out detailed chemical reaction pathways from various configurations. We particularly focus on the time-dependent dissociative adsorption of H₂ near graphene surfaces with a view to engineering applications. The dynamic behavior of dissociative adsorption of an H₂ molecule can be treated successfully, overcoming a difficulty to simulate chemical reactions by MD procedures. Consequently, it is confirmed that hydrogen adsorption is enhanced above steric sites of graphene surfaces where the dissociation of H–H is simultaneously activated. Effective catalytic functions in carbon materials are expected to reduce the cost for metallic catalytic agents. The present results are also well confirmed with an experimental observation [Elias, Nair, Mohiuddin, Morozov, Blake, Hal-sall, Ferrari, Boukhvalov, Katsnelson, Geim, and Novoselov (2009)].

2 Theoretical methods of solution

Figure 1 shows a schematic illustration of our theoretical model in which an H₂ molecule is located above a graphene surface. The present model of graphene consists of 37 C and 15 H atoms, in which C atoms at edges of graphene are passivated by H atoms. As shown in Fig. 1(b), some atoms emphasized as C1, H1, and H2 are featured due to steric conformations of the C and H atoms considered to be effective for the dissociative adsorption of H₂ above graphene surfaces. It is known that H atoms mainly interact with C atoms at the on-top site [Jeloaica and Sidis (1999); Sha and Jackson (2001)]. In this study, a graphene layer is modeled by C₃₇H₁₅, not by a coronene-like model (C₂₄H₁₂). Using this model, the system becomes symmetric around a centrally located C atom and the effect of edges can be reduced. On the other hand, by the use of coronene-like model, the symmetric structure cannot be maintained and the second-neighbor C atoms are located at the edges. It is expected that reactions of an H₂ molecule can be evaluated more accurately above the present model than above coronene-like models. A coupling procedure of *ab initio* methods and MD computations is applied to the dissociative adsorption process of an H₂ molecule above a graphene layer. This is one of the

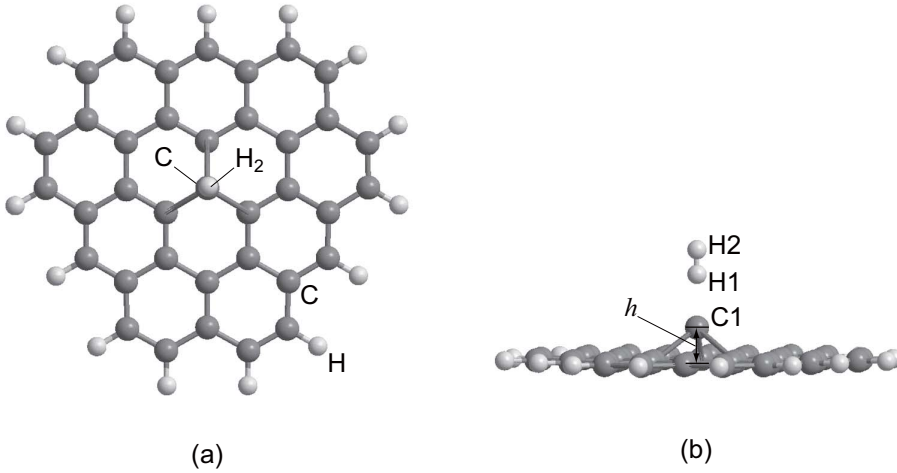


Figure 1: Schematic illustrations of computational models in which an H_2 molecule is located above a model graphene surface of $C_{37}H_{15}$: (a) top view of the system and (b) side view of distorted graphene in which the central C1 atom is elevated at a height h ; the H_2 molecule consists of H1 and H2.

most effective procedures for investigating reaction dynamics induced by electron transfers between activated atoms.

The Hartree–Fock (HF) approximation which requires wave function convergences is employed to the *ab initio* MD simulations. It is important to consider the behavior of wave functions with a high accuracy when reactions are dominated by charge transfer. Furthermore, polyatomic molecular systems have many degrees of freedom and it is difficult to elucidate the reaction pathways fully by static energetical analyses. Therefore, we perform a dynamic analysis on the reaction system using an *ab initio* MD method in which the Lagrangian of the system is written as [Leforestier (1978); Deumens, Diz, Longo, and Öhrn (1994)]:

$$L(\{\mathbf{R}_i\}, \{\dot{\mathbf{R}}_i\}) = \sum_i^N \frac{1}{2} M_i \dot{\mathbf{R}}_i^2 - E_{\text{HF}}(\{\mathbf{R}_i\}, \{\psi_k\}), \quad (1)$$

where \mathbf{R}_i and $\dot{\mathbf{R}}_i$ respectively denote the position and velocity of the i th nucleus, M_i the nuclear mass, and ψ_k an electron wave function of the k th eigenstate. Each electron is quantized and settles in discrete eigenstates. The electronic contributions are calculated in the framework of HF approximation. The potential energy E_{HF} includes nuclear repulsions, nucleus–electron and electron–electron interactions. From Eq. (1), the equation of motion of the i th nucleus is derived

as $M_i \ddot{\mathbf{R}}_i = -\partial E_{\text{HF}}/\partial \mathbf{R}_i$. Considering quantum mechanical contributions to atomic motions, the gradient of E_{HF} is calculated based on the Hellmann–Feynman theorem [Feynman (1939)]. The Hamiltonian of a system is derived from Eq. (1) and is given by [Leforestier (1978); Deumens, Diz, Longo, and Öhrn (1994)]

$$H(\{\mathbf{R}_i\}, \{\mathbf{P}_i\}) = \sum_{i=1}^N \frac{\mathbf{P}_i^2}{2M_i} + E_{\text{HF}}(\{\mathbf{R}_i\}, \{\psi_k\}), \quad (2)$$

where \mathbf{P}_i is the momentum of the i th nucleus. The Hamiltonian is conserved during the computation, *i.e.*, $\dot{H} = 0$. Electrons that contribute to atomic forces are always in the ground state and never break the adiabatic approximation. The unrestricted HF method is employed for open-shell structures such as $\text{C}_{37}\text{H}_{15}$ and $\text{C}_{37}\text{H}_{15}+\text{H}_2$. Electronic structures are obtained using the GAUSSIAN 03 computational code [Frisch (Trucks)]. Electrons in a function space are expanded in terms of a linear combination of atomic orbitals. Pople’s 3–21G(d,p) basis set is employed for the present simulations and 6–31G(d,p) basis set is used for potential energy analyses. For the validation of *ab initio* MD simulation, the normal vibration of H_2 is evaluated by Fourier analysis for the periodic vibration. As a result, a spectrum of normal vibration mode can be obtained and its value corresponds to 53.53 kJ/mol. The experimental value is known to be 50.96 kJ/mol [Witmer (1926)]. The computational result slightly overestimates the experimental data but have a considerable agreement with it. The other well-known techniques in the procedures were reported in previous studies [Kawano (1998); Doi, Haga, Shintaku, and Kawano (2010)]. Integrals of the equation of motion are performed using the velocity Verlet algorithm [Allen and Tildesley (1989)]. The simulation time step is set to 0.5 fs. A time step should be chosen properly for efficient electronic structure computations and for maintaining the conservation laws, although excessively short time steps will prevent long period simulations. The present value of time step is confirmed to conserve the total Hamiltonian of the present system well. The criteria of energy convergence are set to 2.62×10^{-7} kJ/mol. In the *ab initio* MD computations, errors in the total energy are estimated as 0.2 % for 1 ps simulations. Temperature is assumed to be 0 K at initial conditions. Therefore, momentum distributions and thermal effects are not considered in the present simulations. A main purpose is to demonstrate an advantage of this method to find out reaction pathways efficiently. Although computational results strongly depend on the initial configurations, a continuous reaction of dissociative adsorption of H_2 can be clarified by this method and additional potential surface analyses. However, the evaluation of free energies depending on temperature and other experimental conditions is our future work.

3 Results and Discussion

3.1 Preliminary study on *ab initio* MD

Before discussing the *ab initio* MD results, we present a fundamental analysis from the viewpoints of both quantum mechanical and classical mechanical approaches. Figure 2 shows potential energy curves depending on the interactions between an H atom and a planar graphene surface. Here, H1 is located above an on-top site of C1 which is located at the center of graphene, as shown in Fig. 1. A difference in atomic interactions which cause different pictures between *ab initio* MD and classical MD simulations is described later. In Fig. 2, the abscissa is a distance between C1 and H1. The potential energy curves obtained with and without quantum mechanical considerations exhibit quite different characteristics. A curve which was obtained by considering quantum effects had an energetically stable point at 1.15 Å and the dissociation energy of H atom from the graphene was 96.0 kJ/mol. This value is in reasonable agreement with the previous work [Sha and Jackson (2001)]. However, the dissociation limit of the interaction does not converge due to a constraint of the HF approximation. Our main purpose is to perform faster *ab initio* MD computations to search for chemical reaction pathways which are enhanced by charge transfer. More accurate analyses on the electronic structures for the dissociation limits are beyond the scope of this study. On the other hand, without quantum mechanical considerations, H1 which approaches the graphene surface experiences weak attractive forces and it will find a physically stable point near the surface. The dissociation energy of this interaction was evaluated as 1.78 kJ/mol at a distance of 3.05 Å. This weak interaction is caused by the intermolecular force and is well fitted by the following Lennard–Jones type potential:

$$V(r) = 31.3 \left[\left(\frac{2.61}{r} \right)^7 - \left(\frac{2.61}{r} \right)^6 \right]. \quad (3)$$

In this case, the attractive interaction of C1–H1 bond is proportional to $1/r^6$ and it is dominated by the van der Waals interaction. Note that a difference between the curves in Fig. 2 is caused by the different descriptions of electronic motions. In the classical mechanical framework, the atomic force is derived from the gradient of electrostatic potentials of ions, where the electronic distributions do not directly contribute to the interactions. In contrast, in the quantum mechanical approach, electronic distributions vary with the transformation of molecular structures, since the behavior of electrons is explicitly treated on the basis on electrostatic interactions. Figure 2 clearly reveals that the strong C1–H1 bond is caused by electron transfers.

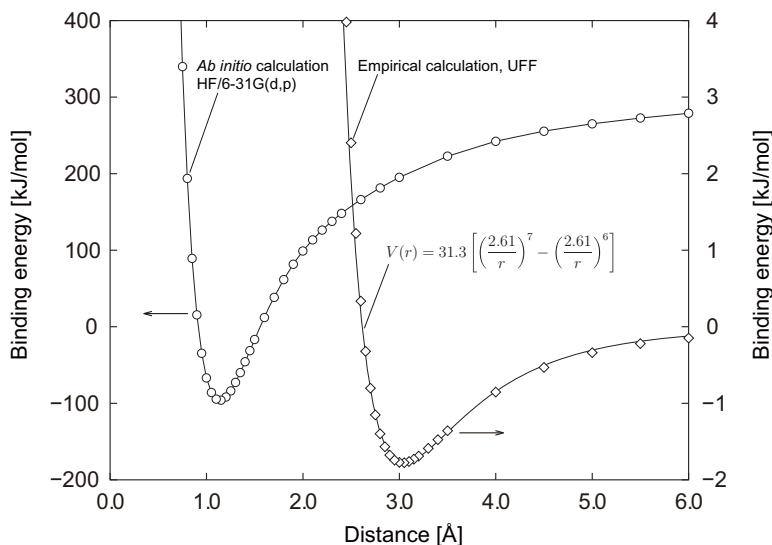


Figure 2: Potential energy curves of an H atom above the central C atom in a graphene layer of $C_{37}H_{15}$ calculated using *ab initio* methods by HF approximation, empirical methods using universal force field (UFF), and Lennard-Jones type potential.

3.2 *Ab initio* MD results for dissociative adsorption of H_2

In this section, results of *ab initio* MD simulations for dissociative adsorption of H_2 above a graphene surface are discussed. Table 1 shows the computational results for different initial conditions. The initial conditions given in Tab. 1 are prepared for twelve cases of **a–l** from infinite number of conditions. In the present computations, initial momenta of the system are set to zero, since this study gives the first step to clarify the nature of phenomenon. Therefore, the results appear to be affected by the initial molecular structures. The possibility of H_2 adsorption on planar and steric graphene surfaces was investigated. In the case of steric surface, C1 which was centrally located in the graphene was elevated above the plane by a height h , as shown in Fig. 1(b). The height h was set to 1.0 Å to enhance H_2 dissociative adsorption. The molecular axis of H_2 was perpendicular or parallel to the surface. The bond lengths of H_2 were set to 0.75 and 1.20 Å for representing an equilibrium structure and an excessively stretched structure, respectively. For both the planar and the steric surfaces, the center of mass of an H_2 molecule was located at 2.0 Å above C1 in the case of **a–h**, and H1 was located at 2.0 Å directly above C1 in the case of **i–l**. In the case of **e–l** in which an H_2 molecular axis was parallel

to the graphene surface, the H1–H2 axis was located above one of C1–C axes. As a result, adsorption of an H atom due to H₂ dissociation was observed only in the case of **d**. Neither dissociation nor adsorption were observed in the other cases: **a–c** and **e–l**. The present results indicate that several conditions have to be satisfied simultaneously to induce the dissociative adsorption of H₂ as shown in the case of **d**. In particular, the H1–H2 bond should be stretched excessively and be near to the graphene surface; the molecular axis of H₂ should be perpendicular to the surface; a steric configuration of C atoms is required to create the adsorption sites. In addition, the present results suggest that parallel conformations of H₂ to the graphene surfaces are not suitable for promoting dissociative adsorption of H₂. However, these limited results could elucidate only a few cases in all possibilities. Therefore, more details about other conformations and other conditions should be investigated in our continuous works. Hereafter, discussions are concentrated on the cases **a–d** in which an H1–H2 axis is perpendicular to the graphene surfaces to elucidate the nature of the phenomenon in detail.

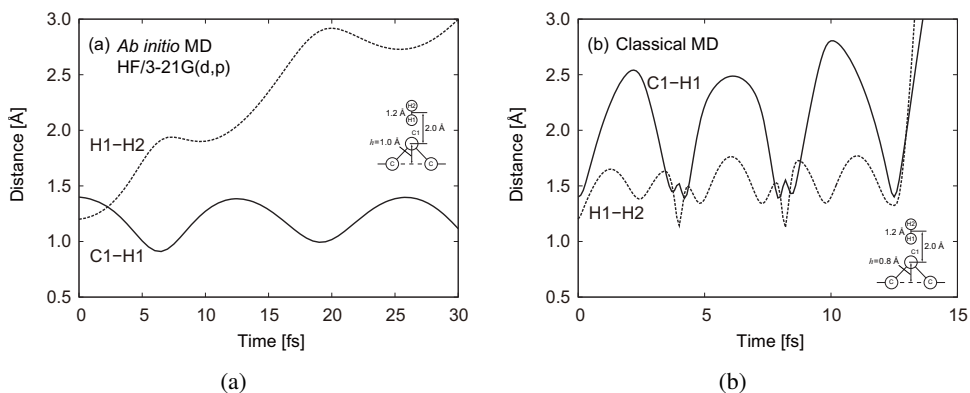


Figure 3: Transitions in the C1–H1 bond length (solid line) and dissociated H1–H2 length (dashed line) obtained using (a) *ab initio* MD with HF/3-21G(d,p) method for initial condition **d** and (b) classical MD for initial condition **d** with substitution of elevated height $h = 0.8 \text{ \AA}$ of C1.

Figure 3 shows transitions of H1–H2 and C1–H1 lengths which promote the dissociative adsorption of H₂. This result was obtained using the initial condition of **d**. As shown in Fig. 3(a), the C1–H1 length oscillates periodically and the H2 atom leaves the graphene layer as time progresses. In this case, the H₂ molecule seems to be activated sufficiently to break H1–H2 bond at the initial condition and to promote adsorption of H1 to C1. A reaction pathway will be clarified by the potential energy surface analysis later. For comparison, a classical MD simulation

was carried out under the similar conditions as the *ab initio* MD simulations. In this case, the height h of C1 was initially set to 0.8 Å from the surface and the H₂ molecule was in the same condition as **d**. When C1 was located at 1.0 Å above the surface (i.e., the same value as for condition **d** in Tab. 1), the graphene layer became too unstable to maintain the structure (this figure is omitted). This instability is mainly caused by the different potential functions used in the *ab initio* MD and in the classical MD. In the present classical MD, the universal force field (UFF) [Rappé, Casewit, Colwell, Goddard III, and Skiff (1992)] was employed for atomic interactions. Consequently, the H₂ molecule bounces above C1 and neither H nor H₂ adsorb on the graphene surface, as shown in Fig. 3(b). Therefore, the dissociative adsorption of H₂ on graphene surfaces should be simulated using advanced MD methods coupling with quantum chemical methods. However, other methods in which the effect of electron transfer is considered empirically have been developed and their progresses are expected to treat chemical reaction systems efficiently [Warshel and Weiss (1980); Schmitt and Voth (1998)]. The results shown in Figs. 3 reveal a drastic difference between the *ab initio* MD and the classical MD calculations. Therefore, the *ab initio* MD method which considers time-dependent electronic motions is very effective to investigate the elementary process of dissociative adsorption of molecules, even though it constrains a short time step and consumes a long computational time.

Figures 4–6 show sequential snapshots of computational results for the conditions of **b**, **c**, and **d**, respectively. In the case of **b** as shown in Fig. 4, above the planar graphene surface, an H₂ molecule dissociated from the surface. At the initial condition of $t = 0$ s, the distance of H1–H2 was set to 1.20 Å and that of C1–H1 to 1.40 Å. Regardless of the excessively stretched H1–H2 bond, the H₂ and the graphene repulsively interacted with each other. In the case of **a**, the result showed similar tendency with that of **b**. Therefore, the details about **a** are omitted here. Figure 5 shows the behavior of H₂ on the steric graphene surface corresponding to the case **c**. In this case, at the initial condition, C1 was elevated at 1.0 Å from the planar surface; the length of H1–H2 was set to 0.75 Å; the distance between C1 and H1 was 1.63 Å. As time progressed, C1 appeared to be attracted by the graphene which maintained the planar structure. On the other hand, the H₂ molecule repulsively dissociated from the surface. In addition, its bond length of 0.75 Å was almost the optimized length and then the vibration between H1 and H2 was little activated. Figure 6 shows the result of condition **d** in which the dissociative adsorption of H₂ was successfully observed. In this case, an excessively stretched H₂ molecule was located above the steric graphene surface. As shown in Fig. 6(b) at $t = 10$ fs, the H1–H2 bond was cleaved due to the attractive interaction between H1 and C1. After that, H1 adsorbed on the graphene as C1 was pulled to the graphene

Table 1: Twelve samples of initial conditions and results of *ab initio* MD computations.

Type	Configuration*	Structure	h [Å]	H1–H2 length [Å]	C1–H1 length [Å]	Result
a	perpendicular	planar	0.0	0.75	1.63	Not adsorbed
b	perpendicular	planar	0.0	1.20	1.40	Not adsorbed
c	perpendicular	steric**	1.0	0.75	1.63	Not adsorbed
d	perpendicular	steric**	1.0	1.20	1.40	Adsorbed
e	parallel†	planar	0.0	0.75	2.00	Not adsorbed
f	parallel†	planar	0.0	1.20	2.00	Not adsorbed
g	parallel†	steric**	1.0	0.75	2.00	Not adsorbed
h	parallel†	steric**	1.0	1.20	2.00	Not adsorbed
i	parallel‡	planar	0.0	0.75	2.00	Not adsorbed
j	parallel‡	planar	0.0	1.20	2.00	Not adsorbed
k	parallel‡	steric**	1.0	0.75	2.00	Not adsorbed
l	parallel‡	steric**	1.0	1.20	2.00	Not adsorbed

* H1–H2 axis is perpendicular or parallel to the graphene surface.

** C1 is elevated from the planar graphene surface.

† The center of mass of H₂ is directly above C1 and H1–H2 axis is located above one of C1–C axes.

‡ H1 is on-top site of C1 and H1–H2 axis is located above one of C1–C axes.

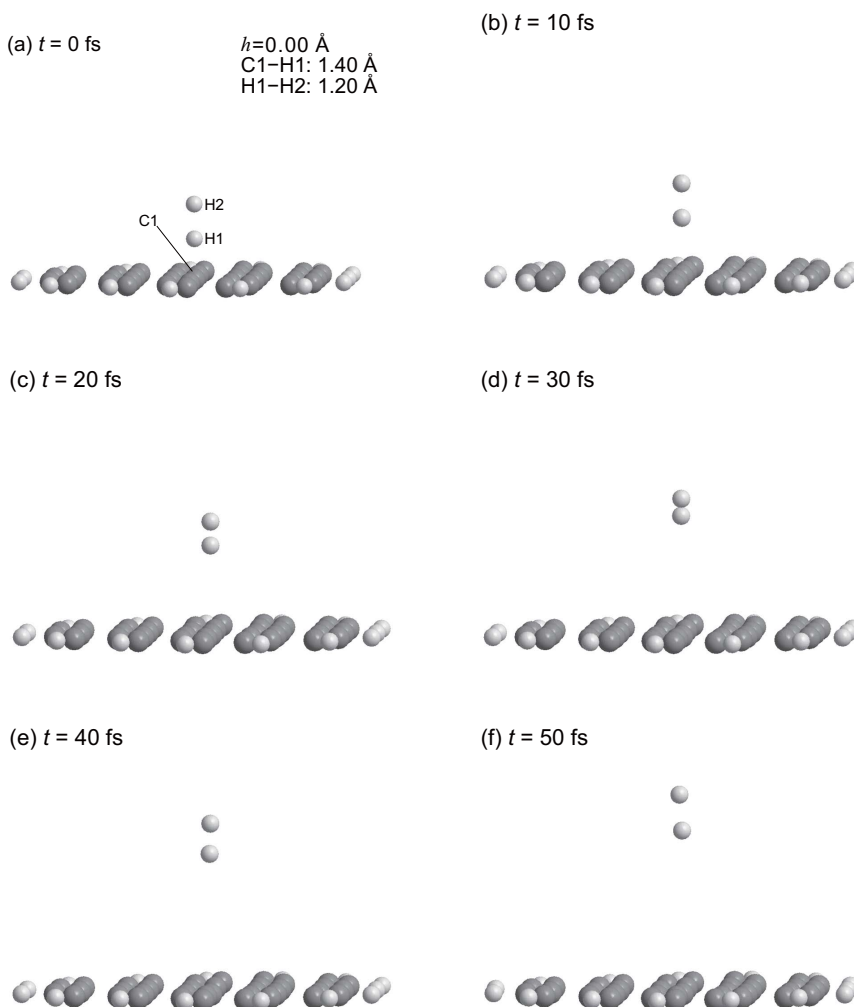


Figure 4: Snapshots of *ab initio* MD simulation with HF/3-21G(d,p) method for initial condition **b** in which h is 0.00 \AA , C1–H1 length is 1.40 \AA , and H1–H2 length is 1.20 \AA : (a) 0 s, (b) 10 fs, (c) 20 fs, (d) 30 fs, (e) 40 fs, and (f) 50 fs.

layer. On the other hand, H2 dissociated from H1 and C1 repulsively. These results mentioned above can be analyzed quantitatively in terms of the Mulliken atomic charge and the bond lengths. Figure 7(a) shows the transitions of C1–H1 and H1–H2 lengths and of Mulliken charges of C1, H1, and H2, in the case of **b**. It is clarified that the H_2 molecule those vibration is excited leaves from the graphene.

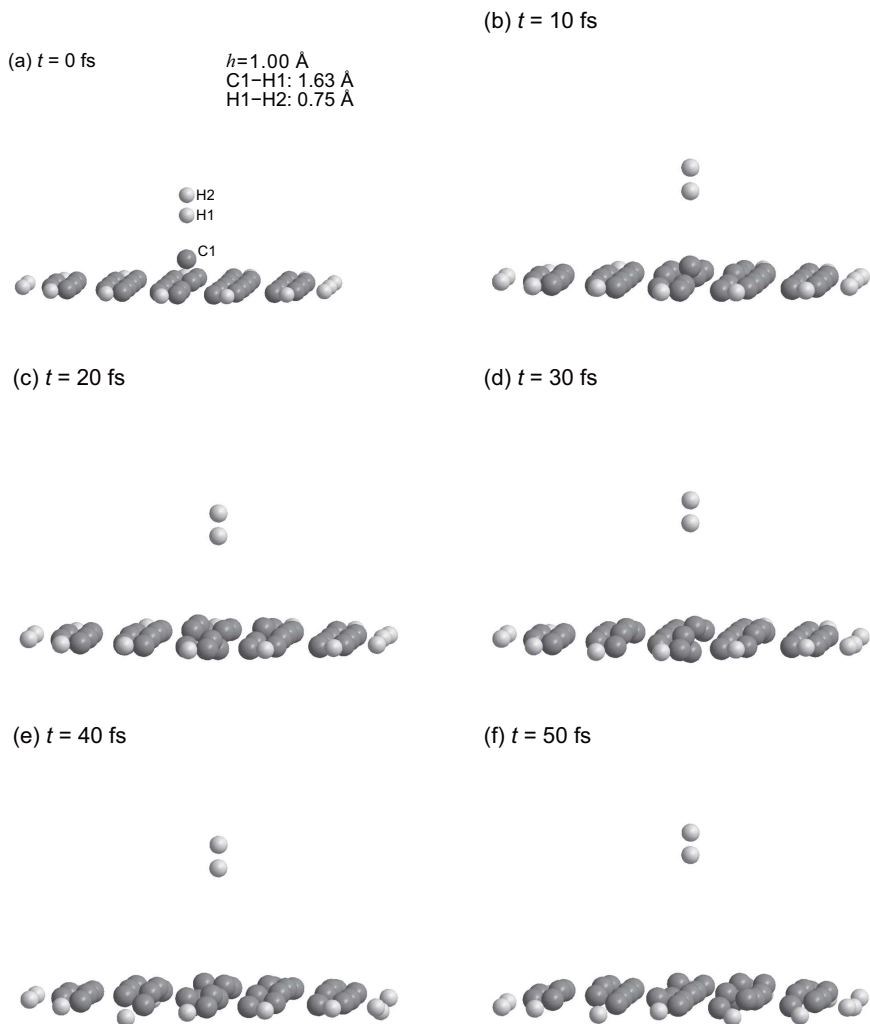


Figure 5: Snapshots of *ab initio* MD simulation with HF/3-21G(d,p) method for initial condition **c** in which h is 1.00 \AA , C1–H1 length is 1.63 \AA , and H1–H2 length is 0.75 \AA : (a) 0 s, (b) 10 fs, (c) 20 fs, (d) 30 fs, (e) 40 fs, and (f) 50 fs.

C1 negatively charged at the initial state turns to be positive as the H_2 molecule dissociates from the surface. On the other hand, positive charges on H1 decrease as time progresses. The H_2 molecule and the graphene appear to be polarized to stabilize their electronic state at the initial condition. However, the charges begin to transfer through those atoms in order to make the system more stable as soon

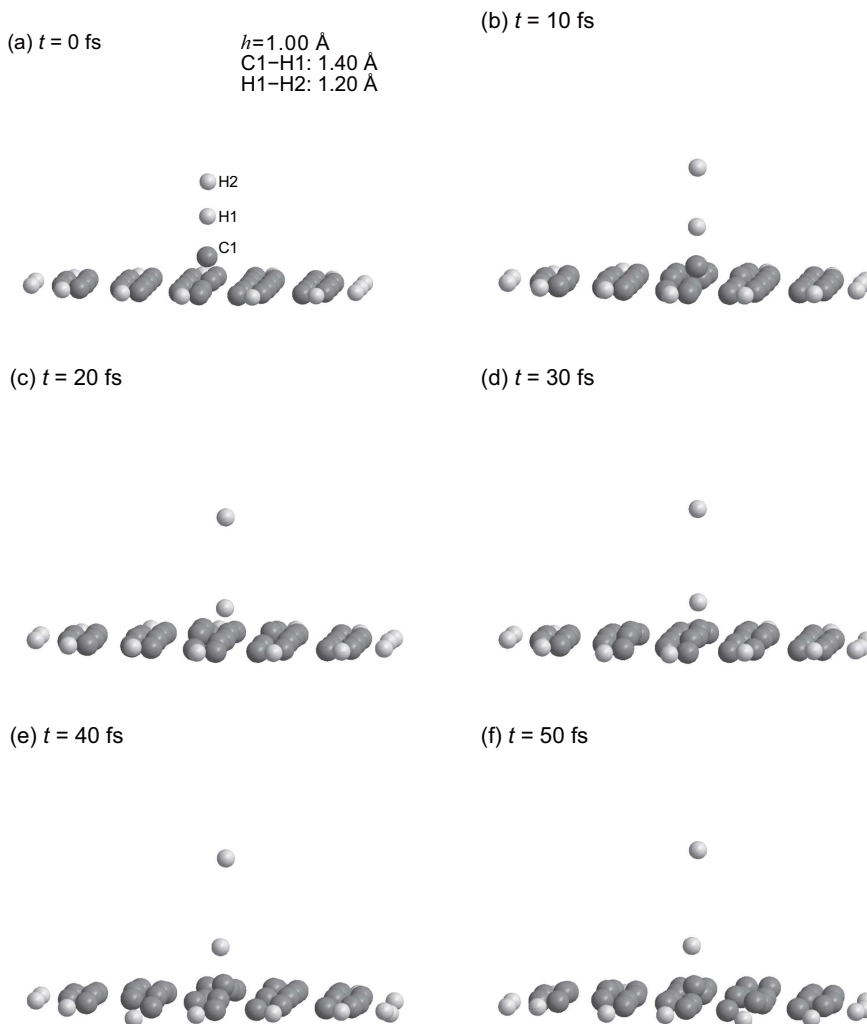


Figure 6: Snapshots of *ab initio* MD simulation with HF/3-21G(d,p) method for initial condition **d** in which h is 1.00 Å, C1–H1 length is 1.40 Å, and H1–H2 length is 1.20 Å: (a) 0 s, (b) 10 fs, (c) 20 fs, (d) 30 fs, (e) 40 fs, and (f) 50 fs.

as the system is released. As time progressed, the polarization between C1, H1, and H2 tends to be depolarized. Therefore, chemical reactions such as dissociative adsorptions of H₂ cannot be expected in this system. Figure 7(b) shows the result of case **c** in which the H₂ molecule is almost optimized. Therefore, the charge transfer through H1 and H2 is little. The distance between C1 and H1 increases

monotonically, regardless of the behavior of C1 which is affected by the nearby C atoms. The charge transfer between C1 and H₂ is not so remarkable that chemical reactions cannot be observed. On the other hand, in the case of **d** as shown in Fig. 7(c), different characteristics from those in Figs. 7(a) and (b) can be obtained due to charge transfer which induces the chemical reaction. In this case, C1 and H1 are polarized at the initial condition, although H2 is almost neutral. As time progresses, H1 becomes more positive and the periods of charge transfer between C1 and H1 appear to synchronize with each other according to the stretching vibration of C1–H1. The period can be roughly estimated to be 11 fs and the length of C1–H1 is averagely maintained at 1.20 Å. In particular, the maximum and minimum points of atomic charge of adsorbed H1 approximately coincide with the peak points of C1–H1 length. This result implies that electrons move from the graphene to the adsorbed H1 atom as the C1–H1 length stretches and that the Mulliken charge shows peaks at the points where the C1–H1 bond length is maximized. Time-averaged values for the atomic charge are 0.231 and –0.282 for H1 and C1, respectively. Generating the C1–H1 bond, H2 turns to be neutral and separate from H1 and C1. It is found that the H1–H2 bond is cleaved slowly different from the separation of H₂ from the graphene surface as shown in Figs. 7(a) and (b). These results indicate that the charge transfer correlates with molecular vibrations and that these electrons play an important role in the intramolecular interactions. On the other hand, the intermolecular dynamics which are not affected by charge transfer and chemical reactions can be described in the framework of conventional MD methods [Kawano (1998); Doi, Haga, Shintaku, and Kawano (2010); Allen and Tildesley (1989)]. The present result in Fig. 7(c) successfully demonstrates a typical characteristic of chemical reactions enhanced by charge transfer.

Figure 8 shows sequential snapshots of a molecular orbital observed in the initial stage of dissociative adsorption of an H₂ molecule for the condition **d**. Isosurfaces of the electron wave function are presented in addition to the atomic positions. Electronic elementary steps in the early period can be discussed from this figure. In the initial condition as shown in Fig. 8(a), an electron is separately observed on the H₂ molecule and the graphene surface. As shown in Figs. 8(b)–(d), the electronic distribution on the H₂ molecule transfers to the graphene side as the H₂ approaches C1 of the graphene. The behavior of charge transfer which synchronizes with the periodic vibration of C1–H1 bond is observed in the first 10 fs. Figures 7(c) and 8 reveal charge transfer which generates repulsive force between H1 and H2 and then the repulsive interaction triggers the dissociation of H1–H2 bond. On the other hand, a chemical bond is formed between the H1 and C1 atoms due to the transferred electrons and due to the polarization between them. Depending on the distance between H1 and C1, the electronic distribution is stabilized instan-

taneously and appears to be synchronized with the vibration. This is an overview of the dynamic process of dissociative adsorption of an H_2 molecule above graphene surface.

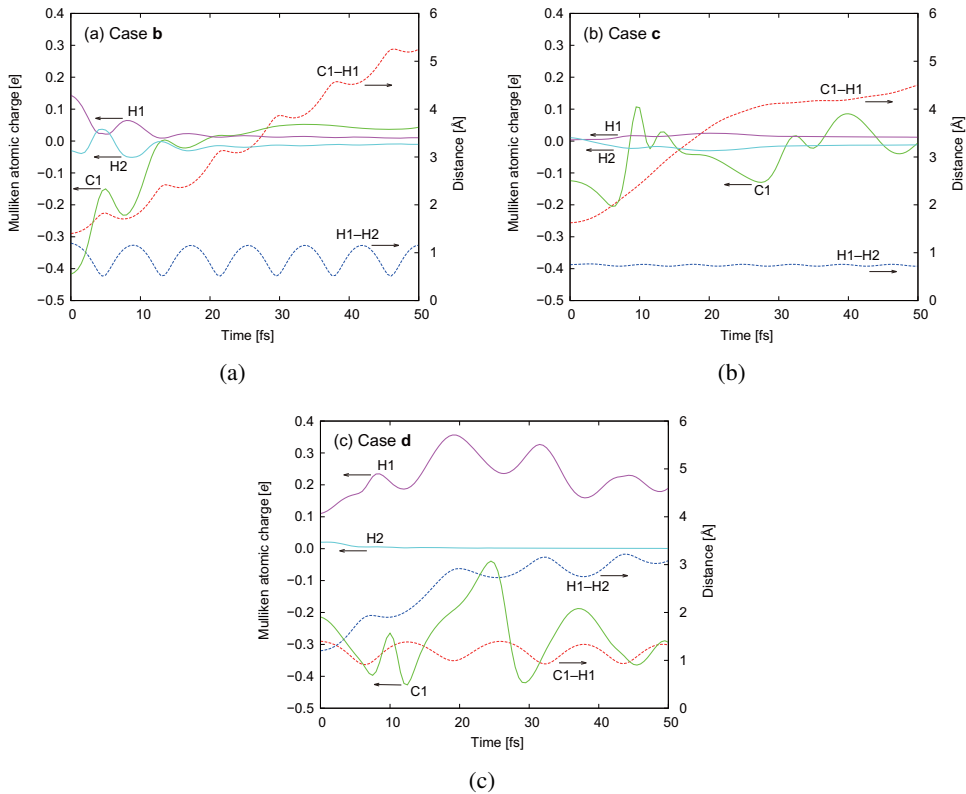


Figure 7: Transitions of Mulliken atomic charge of C1, H1, and H2 (solid lines) and of C1–H1 and H1–H2 lengths (dashed lines) for initial conditions of (a) **b**, (b) **c**, and (c) **d**.

Figures 7 and 8 describe the dynamic process of dissociative adsorption of an H_2 molecule as follows. First, electrons on the H_2 molecule move toward the graphene surface, inducing polarization between the H_2 molecule and the graphene. Second, repulsive interactions are enhanced between the H1 and H2 atoms, which have weakly positive charges (see Fig. 7(c)). On the other hand, the C1 atom which accepts electrons from the H_2 molecule, attracts one of the H atoms and forms a chemical bond with H1. Third, the electrons on C1 move back to H1 after the C1–H1 bond shrinks (see Figs. 7(c) and 8). Finally, the H2 atom located furthest side from the graphene surface leaves in an electrically neutral condition. In this period,

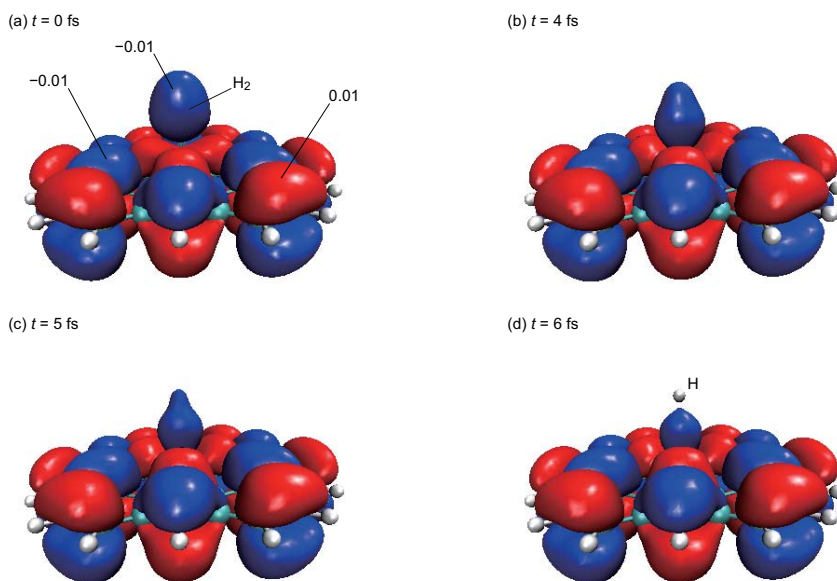


Figure 8: Snapshots of a molecular orbital which focuses on H_2 during *ab initio* MD simulation with HF/3-21G(d,p) method at (a) 0 s, (b) 4.0 fs, (c) 5.0 fs, and (d) 6.0 fs; isosurfaces of the molecular orbital correspond to the values of 0.01 and -0.01.

the positively charged H_2 seems to receive electrons from the negatively charged C1. The periodic vibration between the adsorbed H1 and C1 atoms is conserved due to the periodic charge transfer between them.

In the present study, the existence of a critical pathway in the dissociative adsorption of an H_2 molecule on a graphene layer was suggested as a result of many trials. In a precise sense, all possible trajectories which depend on the initial conditions, temperature, and pressure should be investigated. However, there are many difficulties to satisfy the actual experimental conditions. The present study has found out one of important results in all possibilities. The knowledges obtained from the simulations are very meaningful and motivate more detailed investigations, even though they are resulted from the excessively excited conditions. In the next section, the potential energy surface (PES) analysis is performed to clarify a whole reaction pathway which was partly found out by *ab initio* MD simulations.

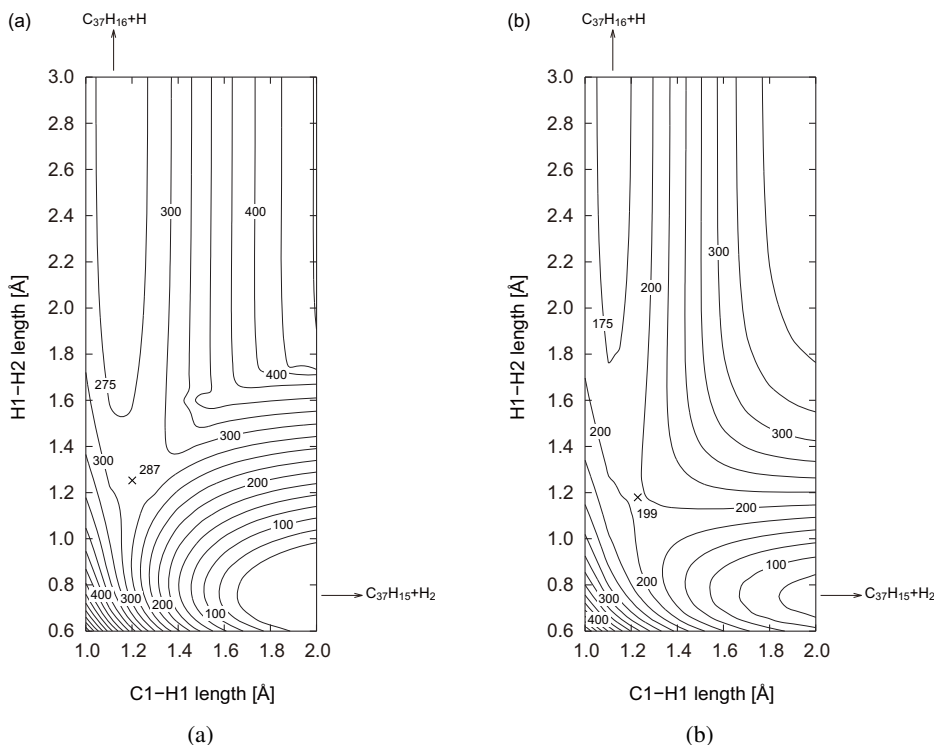


Figure 9: Potential energy surface of H_2 molecule above (a) planar graphene ($h = 0.0 \text{ \AA}$) and (b) steric site on graphene ($h = 0.25 \text{ \AA}$), in which the saddle points are indicated by \times at the location of (a) $(x,y) = (1.20, 1.25)$ and (b) $(x,y) = (1.23, 1.18)$; x and y axes represent C1–H1 length and H1–H2 length, respectively. Values written in the unit of kJ/mol are measured from the reference state of $C_{37}H_{15}+H_2$.

3.3 Potential energy analysis on the reaction pathway

In this section, the validity of the *ab initio* MD results for condition **d** is discussed and critical reaction pathways will be elucidated according to the manner of quantum chemistry. A purpose of this section is to explain the nature of dissociative adsorption of H_2 on graphene surfaces. The PESs for the static system between $C_{37}H_{15}+H_2$ and $C_{37}H_{16}+H$ were investigated. In this analysis, the 6-31G(d,p) basis set was adopted instead of the 3-21G(d,p) basis set which was used for the *ab initio* MD computations. It is for the higher accuracy and for the quantitative comparison with the previous works [Elias, Nair, Mohiuddin, Morozov, Blake, Halsall, Ferrari, Boukhalov, Katsnelson, Geim, and Novoselov (2009); Sha and Jackson

(2001)]. The difference of basis sets was confirmed to be less effective for the H_2 dissociation process. However, the dissociative adsorption process of an H_2 molecule was limited near a graphene surface where electron transfers between the two molecules induced the reaction, because the dissociation limit on a continuous PES should not be discussed by the HF approximation. Figure 9 shows the contour maps of the relative potential energy with respect to interactions between an H_2 molecule and a graphene surface as a function of C1–H1 and H1–H2 lengths. The relative energies were measured from the isolated condition of an H_2 molecule and a graphene: $C_{37}H_{15}+H_2$. The C1 atom located at the center of graphene was elevated from the planar surface by $h = 0.25 \text{ \AA}$ as well as the case of $h = 0 \text{ \AA}$. Although this height is lower than that of condition **d**, it seems to be more realistic [Elias, Nair, Mohiuddin, Morozov, Blake, Halsall, Ferrari, Boukhvalov, Katsnelson, Geim, and Novoselov (2009); Sha and Jackson (2001)] from the viewpoint of stability. Figure 9(a) shows the contour map of the case of $h = 0 \text{ \AA}$. It is found that there are steeps along the directions to shorten the C1–H1 length and to stretch the H1–H2 length and that an H_2 molecule located far from the graphene surface is stable. A cross mark in the map is considered to be a saddle point in the reaction pathway between $C_{37}H_{15}+H_2$ and $C_{37}H_{16}+H$. The energy difference between the dissociation limit of $C_{37}H_{15}+H_2$ and the saddle point shows that an activation energy of 287 kJ/mol (2.98 eV) is required to cleave an H_2 molecule. On the other hand, the other local minimum of $C_{37}H_{16}+H$ is very shallow and gradients around it are moderate. This result means that quite-high energy should be provided to cleave the H1–H2 bond and that the excessively high energy will negatively contribute to the repulsion between the H atoms and the graphene. Therefore, it will be difficult to realize the dissociative adsorption of H_2 molecules on planar graphene surfaces. Figure 9(b) shows the result about the case of $h = 0.25 \text{ \AA}$, that is, the case of steric graphene surface. It is found that gradients around the stable state of $C_{37}H_{15}+H_2$ appear to be more moderate than those in Fig. 9(a). The energy required to cleave the H1–H2 bond evaluated as 199 kJ/mol (2.06 eV). This value is 88 kJ/mol (0.92 eV) lower than the activation energy is evaluated on the planar graphene surface. These moderate gradients enable the successive dissociation and adsorption of H_2 . Additionally, the saddle points in the other cases of $h = 0.50$, 0.75, and 1.00 \AA were evaluated as 252 kJ/mol (2.61 eV), 450 kJ/mol (4.66 eV), and 760 kJ/mol (7.88 eV), respectively, although their PESs are omitted here. It is predicted that the activation energy increases as h increases and that infinitesimal distortions of graphene surfaces are effective to decrease the activation energy of H_2 dissociation. In comparison with the present result, the dissociation energy of an H_2 molecule in vacuum without graphene was estimated here to be 354 kJ/mol (3.67 eV), which was in reasonable agreement with the experimental value of 432 kJ/mol (4.48 eV) [Herzberg (1969)]. That is, in the case of $h = 0.25 \text{ \AA}$, the dissoci-

ation energy of H_2 above graphene is estimated as 155 kJ/mol (1.61 eV) lower than that without graphene. Consequently, steric C sites on the graphene surface are expected to act as a catalytic agent. Both previous results for an H atom near a carbon surface [Jeloacia and Sidis (1999)] and the present results for an H_2 molecule strongly indicate the feasibility of using a distorted carbon material for hydrogen storage materials.

In practical applications, external energy estimations are required to form steric sites which distort the planar graphene surface and to move the H_2 molecule toward the surface. More accurate energy estimations will be possible using the density functional theory, the multi-configurational self-consistent field, or the configuration interactions [Szabo and Ostlund (1982)]. However, as a first step, we carried out the present *ab initio* MD analysis to investigate the dissociative adsorption process of H_2 molecules, focusing on the molecular dynamics, the Mulliken atomic charges, and molecular orbitals.

4 Conclusion

In the present study, an *ab initio* MD method with wave function convergences was developed and used to investigate the time-dependent behavior of an H_2 molecule above a graphene surface. The simulations could quantitatively evaluate a scenario in which distorted graphene surfaces enhanced H_2 dissociation and an H atom adsorption at the steric sites. In conjunction with this *ab initio* MD simulations, the potential energy surface analysis was also applied to clarify the detailed dissociative adsorption process of an H_2 molecule. Important conclusions obtained from this study are summarized below.

1. Focusing on dissociative adsorption of H_2 on a graphene surface, the time-dependent phenomena were clarified by the present procedure. In particular, sequential electron transfers from H_2 to C and from C to 2H were indicated. The former process dominated H_2 dissociation and the latter one dominated the subsequent C–H adsorption with the dissociation of a neutral H atom. Furthermore, the periodic electron transfer which was synchronized with the C–H vibration was predicted.
2. Based on the *ab initio* MD results, a critical reaction pathway for the dissociative adsorption was determined. The calculations in the present study suggest that H_2 dissociation can be realized above the distorted graphene surface with an activation energy of 199 kJ/mol (2.06 eV), which is lower than that in vacuum without graphene. However, the same process is not expected to occur on a planar surface because the dissociation limit of $C_{37}H_{15}+H_2$ is

so stable that quite-high energies to induce the dissociative adsorption negatively cause repulsions between H atoms and a graphense surface.

3. The dissociation energy of an H–H bond near the steric configuration of C atoms was expected to be reduced to 56.2 % of that without graphene. This result highlights the capacity of distorted graphene to be available as a catalytic agent which does not require expensive materials such as Pt. Furthermore, by exploiting the subsequent C–H adsorption, steric graphene surfaces are promising candidates for hydrogen storages.

References

- Allen, M. P.; Tildesley, D. J.** (1989): *Computer Simulation of Liquids*.
- Arellano, J. S.; Molina, L. M.; Rubio, A.; Alonso, J. A.** (2000): Density functional study of adsorption of molecular hydrogen on graphene layers. *J. Chem. Phys.*, vol. 112, pp. 8114–8119.
- Bersth, P. A.; Harter, A. G.; Zidan, R.; Blomqvist, A.; Araújo, C. M.; Scheicher, R. H.; Ahuja, R.; Jena, P.** (2009): Carbon nanomaterials as catalysts for hydrogen uptake and release in NaAlH₄. *Nano Lett.*, vol. 9, pp. 1501–1505.
- Chan, S.-P.; Chen, G.; Gong, X. G.; Liu, Z.-F.** (2001): Chemisorption of hydrogen molecules on carbon nanotubes under high pressure. *Phys. Rev. Lett.*, vol. 87, pp. 205502–1–205502–4.
- Chen, P.; Wu, X.; Lin, J.; Tan, K. L.** (1999): High H₂ uptake by alkali-doped carbon nanotubes under ambient pressure and moderate temperatures. *Science*, vol. 285, pp. 91–93.
- Chen, Y.; Shaw, D. T.; Bai, X. D.; Wang, E. G.; Lund, C.; Lu, W. M.; Chung, D. D. L.** (2001): Hydrogen storage in aligned carbon nanotubes. *Appl. Phys. Lett.*, vol. 78, pp. 2128–2130.
- Cheng, H.; Pez, G.; Kern, G.; Kresse, G.; Hafner, J.** (2001): Hydrogen adsorption in potassium-intercalated graphite of second stage: an *ab initio* molecular dynamics study. *J. Phys. Chem. B*, vol. 105, pp. 736–742.
- Cheng, H.; Pez, G. P.; Cooper, A. C.** (2003): Spontaneous cross linking of small-diameter single-walled carbon nanotubes. *Nano Lett.*, vol. 3, pp. 585–587.
- Deumens, E.; Diz, A.; Longo, R.; Öhrn, Y.** (1994): Time-dependent theoretical treatments of the dynamics of electrons and nuclei in molecular systems. *Rev. Mod. Phys.*, vol. 66, pp. 917–983.

Dillon, A. C.; Jones, K. M.; Bekkedahl, T. A.; Kiang, C. H.; Bethune, D. S.; Heben, M. J. (1997): Storage of hydrogen in single-walled carbon nanotubes. *Nature*, vol. 386, pp. 377–379.

Doi, K.; Haga, T.; Shintaku, H.; Kawano, S. (2010): Development of coarse-graining DNA models for single-nucleotide resolution analysis. *Phi. Trans. R. Soc. A*, vol. 368, pp. 2615–2628.

Doi, K.; Nakano, H.; Ohta, H.; Tachibana, A. (2007): First-principle molecular-dynamics study of hydrogen and aluminum nanowires in carbon nanotubes. *Mater. Sci. Forum*, vol. 539–543, pp. 1409–1414.

Durgun, E.; Ciraci, S.; Yildirim, T. (2008): Functionalization of carbon-based nanostructures with light transition-metal atoms for hydrogen storage. *Phys. Rev. B*, vol. 77, pp. 085405–1–085405–9.

Elias, D. C.; Nair, R. R.; Mohiuddin, T. M. G.; Morozov, S. V.; Blake, P.; Halsall, M. P.; Ferrari, A. C.; Boukhvalov, D. W.; Katsnelson, M. I.; Geim, A. K.; Novoselov, K. S. (2009): Control of graphene's properties by reversible hydrogenation: evidence for graphane. *Science*, vol. 323, pp. 610–613.

Feynman, R. P. (1939): Forces in molecules. *Phys. Rev.*, vol. 56, pp. 340–343.

Frisch, M. J.; Trucks, G. W.; Schlegel, H. B.; Scuseria, G. E.; Robb, M. A.; Cheeseman, J. R.; Montgomery Jr, J. A.; Vreven, T.; Kudin, K. N.; Burant, J. C.; Millam, J. M.; Iyengar, S. S.; Tomasi, J.; Barone, V.; Mennucci, B.; Cossi, M.; Scalmani, G.; Rega, N.; Petersson, G. A.; Nakatsuji, H.; Hada, M.; Ehara, M.; Toyota, K.; Fukuda, R.; Hasegawa, J.; Ishida, M.; Naka-jima, T.; Honda, Y.; Kitao, O.; Nakai, H.; Klene, M.; Li, X.; Knox, J. E.; Hratchian, H. P.; Cross, J. B.; Adamo, C.; Jaramillo, J.; Gomperts, R.; Stratmann, R. E.; Yazyev, O.; Austin, A. J.; Cammi, R.; Pomelli, C.; Ochterski, J. W.; Ayala, P. Y.; Morokuma, K.; Voth, G. A.; Salvador, P.; Dannenberg, J. J.; Zakrzewski, V. G.; Dapprich, S.; Daniels, A. D.; Strain, M. C.; Farkas, O.; Malick, D. K.; Rabuck, A. D.; Raghavachari, K.; Foresman, J. B.; Ortiz, J. V.; Cui, Q.; Baboul, A. G.; Clifford, S.; Cioslowski, J.; Stefanov, B. B.; Liu, G.; Liashenko, A.; Piskorz, P.; Komaromi, I.; Martin, R. L.; Fox, D. J.; Keith, T.; Al-Laham, M. A.; Peng, C. Y.; Nanayakkara, A.; Challacombe, M.; Gill, P. M. W.; Johnson, B.; Chen, W.; Wong, M. W.; Gonzalez, C.; Pople, J. A. (2004): computer code GAUSSIAN 03 Rev. D.01, 2004.

Guisiniger, N. P.; Rutter, G. M.; Crain, J. N.; First, P. N.; Stroscio, J. A. (2009): Exposure of epitaxial graphene on SiC(0001) to atomic hydrogen. *Nano Lett.*, vol. 9, pp. 1462–1466.

- Gupta, B. K.; Srivastava, O. N.** (2000): Synthesis and hydrogenation behaviour of graphitic nanofibres. *Int. J. Hydrogen Energy*, vol. 25, pp. 825–830.
- Gupta, B. K.; Srivastava, O. N.** (2001): Further studies on microstructural characterization and hydrogenation behaviour of graphitic nanofibres. *Int. J. Hydrogen Energy*, vol. 26, pp. 857–862.
- Hanasaki, I.; Nakamura, A.; Yonebayashi, T.; Kawano, S.** (2008): Structure and stability of water chain in a carbon nanotube. *J. Phys. Condens. Matter*, vol. 20, pp. 015213–1–015213–7.
- Herzberg, G.** (1969): Dissociation energy and ionization potential of molecular hydrogen. *Phys. Rev. Lett.*, vol. 23, pp. 1081–1083.
- Hirscher, M.; Becher, M.; Haluska, M.; Dettlaff-Weglikowska, U.; Quintel, A.; Duesberg, G. S.; Choi, Y.-M.; Downes, P.; Hulman, M.; Roth, S.; Stepanek, I.; Bernier, P.** (2001): Hydrogen storage in sonicated carbon materials. *Appl. Phys. A*, vol. 72, pp. 129–132.
- Jeloacia, L.; Sidis, V.** (1999): DFT investigation of the adsorption of atomic hydrogen on a cluster-model graphite surface. *Chem. Phys. Lett.*, vol. 300, pp. 157–162.
- Kawano, S.** (1998): Molecular dynamics of rupture phenomena in a liquid thread. *Phys. Rev. E*, vol. 58, pp. 4468–4472.
- Leforestier, C.** (1978): Classical trajectories using the full *ab initio* potential energy surface $\text{H}^- + \text{CH}_4 \rightarrow \text{CH}_4 + \text{H}^-$. *J. Chem. Phys.*, vol. 68, pp. 4406–4410.
- Li, J.; Furuta, T.; Goto, H.; Ohashi, T.; Fujiwara, Y.; Yip, S.** (2003): Theoretical evaluation of hydrogen storage capacity in pure carbon nanostructures. *J. Chem. Phys.*, vol. 119, pp. 2376–2385.
- Liu, C.; Fan, Y. Y.; Liu, M.; Cong, T. H.; Cheng, H. M.; Dresselhaus, M. S.** (1999): Hydrogen storage in single-walled carbon nanotubes at room temperature. *Science*, vol. 286, pp. 1127–1129.
- Miura, Y.; Kasai, H.; Diño, W. A.; Nakanishi, H.; Sugimoto, T.** (2003): First principles studies on the interaction of a hydrogen atom with a single-walled carbon nanotube. *Jpn. J. Appl. Phys.*, vol. 42, pp. 4626–4629.
- Nakano, H.; Ohta, H.; Yokoe, A.; Doi, K.; Tachibana, A.** (2006): First-principle molecular-dynamics study of hydrogen adsorption on an aluminum-doped carbon nanotube. *J. Power Sources*, vol. 163, pp. 125–134.
- Nishimiya, N.; Ishigaki, K.; Takikawa, H.; Ikeda, M.; Hibi, Y.; Sakakibara, T.; Matsumoto, A.; Tsutsumi, K.** (2002): Hydrogen sorption by single-walled

carbon nanotubes prepared by a torch arc method. *J. Alloys Compd.*, vol. 339, pp. 275–282.

Okamoto, Y.; Miyamoto, Y. (2001): *Ab initio* investigation of physisorption of molecular hydrogen on planar and curved graphenes. *J. Phys. Chem. B*, vol. 105, pp. 3470–3474.

Patchkovskii, S.; Tse, J. S.; Yurchenko, S. N.; Zhechkov, L.; Heine, T.; Seifert, G. (2005): Graphene nanostructures as tunable storage media for molecular hydrogen. *Proc. Nat. Acad. Sci. U.S.A.*, vol. 102, pp. 10439–10444.

Rappé, A. K.; Casewit, C. J.; Colwell, K. S.; Goddard III, W. A.; Skiff, W. M. (1992): UFF, a full periodic table force field for molecular mechanics and molecular dynamics simulations. *J. Am. Chem. Soc.*, vol. 114, pp. 10024–10035.

Riedl, C.; Coletti, C.; Iwasaki, T.; Zakharov, A. A.; Starke, U. (2009): Quasi-free-standing epitaxial graphene on SiC obtained by hydrogen intercalation. *Phys. Rev. Lett.*, vol. 103, pp. 246804–1–246804–4.

Riedl, C.; Coletti, C.; Starke, U. (2010): Structural and electronic properties of epitaxial graphene on SiC(0001): a review of growth, characterization, transfer doping and hydrogen intercalation. *J. Phys. D: Appl. Phys.*, vol. 43, pp. 374009–1–374009–15.

Schmitt, U. W.; Voth, G. A. (1998): Multistate empirical valence bond model for proton transport in water. *J. Phys. Chem. B*, vol. 102, pp. 5547–5551.

Sha, X.; Jackson, B. (2001): First-principles study of the structural and energetic properties of H atoms on a graphite (0001) surface. *Surf. Sci.*, vol. 496, pp. 318–330.

Ströbel, R.; Jörissen, L.; Schliermann, T.; Trapp, V.; Schütz, W.; Bohmhammel, K.; Wolf, G.; Garcke, J. (1999): Hydrogen adsorption on carbon materials. *J. Power Sources*, vol. 84, pp. 221–224.

Szabo, A.; Ostlund, N. S. (1982): *Modern Quantum Chemistry*.

Tada, K.; Furuya, S.; Watanabe, K. (2001): *Ab initio* study of hydrogen adsorption to single-walled carbon nanotubes. *Phys. Rev. B*, vol. 63, pp. 155405–1–155405–4.

Virojanadara, C.; Yakimova, R.; Zakharov, A. A.; Johansson, L. I. (2010): Large homogeneous mono-/bi-layer graphene on 6H-SiC(0001) and buffer layer elimination. *J. Phys. D: Appl. Phys.*, vol. 43, pp. 374010–1–374010–13.

Virojanadara, C.; Zakharov, A. A.; Yakimova, R.; Johansson, L. I. (2010): Buffer layer free large area bi-layer graphene on SiC(0001). *Surf. Sci. Lett.*, vol. 604, pp. L4–L7.

Warshel, A.; Weiss, R. M. (1980): An empirical valence bond approach for comparing reactions in solutions and in enzymes. *J. Am. Chem. Soc.*, vol. 102, pp. 6218–6226.

Witmer, E. E. (1926): Critical potentials and the heat of dissociation of hydrogen as determined from its ultra-violet band spectrum. *Proc. Nat. Acad. Sci. U.S.A.*, vol. 12, pp. 238–244.

Xu, W.-C.; Takahashi, K.; Matsuo, Y.; Hattori, Y.; Kumagai, M.; Ishiyama, S.; Kaneko, K.; Iijima, S. (2007): Investigation of hydrogen storage capacity of various carbon materials. *Int. J. Hydrogen Energy*, vol. 32, pp. 2504–2512.

Yang, R. T. (2000): Hydrogen storage by alkali-doped carbon nanotubes-revisited. *Carbon*, vol. 38, pp. 623–641.